THE JOURNAL OF BIOLOGICAL CHEMISTRY VOL. 284, NO. 48, pp. 33151–33160, November 27, 2009

Interaction between the SifA Virulence Factor and Its Host Target SKIP Is Essential for *Salmonella* Pathogenesis*[S]

Received for publication, June 18, 2009, and in revised form, September 16, 2009 Published, JBC Papers in Press, September 28, 2009, DOI 10.1074/jbc.M109.034975

Lautaro Diacovich[‡1], Audrey Dumont[‡2], Daniel Lafitte[§], Elodie Soprano[¶], Aude-Agnès Guilhon[‡], Christophe Bignon[¶], Jean-Pierre Gorvel[‡], Yves Bourne[¶3], and Stéphane Méresse[‡3,4]

From the [‡]Centre d'Immunologie de Marseille-Luminy, CNRS UMR 6102, INSERM U631, Université de la Méditerranée, Parc Scientifique de Luminy, Case 906, 13288 Marseille Cedex 9, the [¶]Architecture et Fonction des Macromolécules Biologiques, UMR 6098, CNRS Université Aix-Marseille, Parc Scientifique de Luminy, Case 932, 13288 Marseille Cedex 9, and the [§]Plateau Protéomique Timone, INSERM UMR 911, Aix-Marseille Université, 13288 Marseille, France

SifA is a *Salmonella* effector that is translocated into infected cells by the pathogenicity island 2-encoded type 3 secretion system. SifA is a critical virulence factor. Previous studies demonstrated that, upon translocation, SifA binds the pleckstrin homology motif of the eukaryotic host protein SKIP. In turn, the SifA-SKIP complex regulates the mobilization of the molecular motor kinesin-1 on the bacterial vacuole. SifA exhibits multiple domains containing functional motifs. Here we performed a molecular dissection and a mutational study of SifA to evaluate the relative contribution of the different domains to SifA functions. Biochemical and crystallographic analysis confirmed that the N-terminal domain of SifA is sufficient to interact with the pleckstrin homology domain of SKIP, forming a 1:1 complex with a micromolar dissociation constant. Mutation of the tryptophan residue in the W*XXX*E motif, which has been proposed to mimic active form of GTPase, deeply affected the stability and the translocation of SifA while mutations of the glutamic residue had no functional impact. A SifA L130D mutant that does not bind SKIP showed a Δ*sifA*-like phenotype both in infected cells and in the mouse model of infection. We concluded that the W*XXX*E motif is essential for maintaining the tertiary structure of SifA, the functions of which require the interaction with the eukaryotic protein SKIP.

Salmonella enterica serovar Typhimurium (*S. typhimurium*)[5] is a Gram-negative enteropathogenic bacterium causing widely distributed food-borne diarrheal infections in humans (1, 2). The virulence of this pathogen relies on its ability to establish a replicative niche, named the *Salmonella*-containing vacuole (SCV), inside host cells. The latter is a dedicated membrane-bound compartment specifically shaped by the activity of several *Salmonella* effector proteins. Indeed, the type 3 secretion systems (T3SS), encoded by *Salmonella* pathogenicity islands 2 (T3SS-2), is used by *Salmonella* to translocate a repertoire of twenty or so effector proteins (3). These T3SS-2 effectors are collectively required for intracellular replication and systemic infection in mice. They are responsible for a large panel of functions that include enzymatic activities (4–6) and cellular processes such as the regulation of vacuolar membrane dynamics (7), interaction with the host cell cytoskeleton (4, 8, 9), and intracellular localization of the SCV (10, 11).

Upon translocation, the T3SS-2 effectors PipB2 and SifA are localized to the SCV and *Salmonella*-induced filaments (Sif) membrane. PipB2 acts as a linker for the plus-end-directed microtubule motor Kinesin-1 and mediates its recruitment (8). SifA interacts with the eukaryotic protein SKIP (SifA and kinesin interacting protein) and regulates the level of kinesin-1 on the SCV (12). We previously showed that either the absence of SifA, in Δ*sifA* mutant, or the absence of SKIP in cells treated with a specific small interference RNA, result in accumulation of kinesin-1 on the *Salmonella* vacuole, thus demonstrating that SifA and SKIP form a functional complex that controls this phenotype. SKIP is a protein of 1020-residue length that possesses at least two distinct functional domains. The N-terminal region contains a RUN motif and interacts with kinesin-1 by a yet unknown process. The C-terminal pleckstrin homology (PH) domain binds to SifA (12). SifA contains two domains, and each includes functional motifs. The N-terminal domain contains conserved amino acid sequences shared by *Salmonella* effectors of the *Salmonella*-translocated effectors group and a well conserved motif (WEK(I/M)*XX*FF) that has been proposed to direct the translocation by T3SS-2 (13). The larger C-terminal domain encloses at least two functional motifs. The C-terminal hexapeptide is lipidated upon translocation (14) and serves as host membrane anchor (15). The W*XXX*E motif is conserved within a 24-member bacterial effector protein family and has been proposed to confer GTPase mimicry activity (16) and to contribute to the function of SifA. The T3SS-2 effector SifB that shares 30% sequence identity with SifA is a member of this bacterial effector family. SifB localizes to SCVs and Sifs, but

* This work was supported by Grant "Equipe FRM" (to S. M.), the ANR (Grant ANR-05-BLAN-0028-01 to Y. B. and S. M.), and institutional grants from CNRS and INSERM.

[S] The on-line version of this article (available at http://www.jbc.org) contains supplemental text, Figs. S1 and S2, and additional references.

The atomic coordinates and structure factors (code 3HW2) have been deposited in the Protein Data Bank, Research Collaboratory for Structural Bioinformatics, Rutgers University, New Brunswick, NJ (http://www.rcsb.org/).

[1] Recipient of a fellowship from the European Molecular Biology Organization.

[2] Recipient of a fellowship from the French Ministry of Research.

[3] Groups of Architecture et Fonction des Macromolécules Biologiques (under Y. B.) and Centre d'Immunologie de Marseille-Luminy (under S. M.) contributed equally to this work.

[4] To whom correspondence should be addressed. Tel.: 33-4-91-269115; Fax: 33-4-91-269430; E-mail: meresse@ciml.univ-mrs.fr.

[5] The abbreviations used are: *S. typhimurium*, *Salmonella enterica* serovar Typhimurium; PH, pleckstrin homology; SCV, *Salmonella*-containing vacuole; Sif, *Salmonella*-induced filament; T3SS, type 3 secretion system; T3SS-2, T3SS encoded by *Salmonella* pathogenicity islands 2; HA, hemagglutinin; GFP, green fluorescent protein; CMV, cytomegalovirus; GST, glutathione *S*-transferase.

its function remains unknown (17). SifA was recently found to interact with GDP-bound RhoA and proposed to have GTPase guanine nucleotide exchange activity, in which the conserved W*XXX*E motif could represent a structural feature (18). Here we report insights into the functional and structural organization of the T3SS-2 SifA effector. We show that the W*XXX*E sequence is a conserved structural motif important for both the folding and the secretion of the SifA effector and that the role of SifA in virulence is mediated by its interaction with the host protein SKIP.

EXPERIMENTAL PROCEDURES

Chemicals, Strains, Plasmids, and DNA Manipulation—The *Salmonella typhimurium* strains used in this work were wild-type 12023 (NTCC) and its isogenic derivatives. The *Salmonella* and *Escherichia coli* strains and plasmids used in this study are listed below in Table 1. Synthetic primers are listed below in Table 2. Ampicillin (100 μg ml^{-1}), chloramphenicol (25 μg ml^{-1}), kanamycin (50 μg ml^{-1}), or Zeocin (50 μg ml^{-1}) were added when required. C41 (DE3) (Avidis) is a BL21 (DE3)-derived strain used to overcome toxic effects associated with protein overexpression (19).

Culture Conditions, Protein Production, and Protein Methods—*E. coli* strains harboring the indicated plasmids were grown at 37 °C in Luria-Bertani medium (Difco, San Jose, CA) supplemented with the corresponding antibiotics. Overnight cultures were diluted 1:100 in fresh medium, Superior Broth (AthenaES) for His_6::SifA, His_6::SifA-(s3015), and His_6::SifA-(s2983) or Turbo Broth (AthenaES) for His_6::SKIP(PH). Optimization of protein expression and solubility was performed as previously described (20).

Antibodies and Reagents—The mouse anti-His_6 (Qiagen), anti-Myc 9E10, anti-HA (clone 16B12, Covance, Richmond, CA), anti-GFP (clone JL-8, Clontech, Mountain View, CA), the rabbit anti-kinesin HC (21), anti-GFP (Molecular Probes, Eugene, OR), and the rat anti-HA (clone 3F10; Roche Molecular Biochemicals, Indianapolis, IN) antibodies were used at a 10^{-3} dilution. The mouse monoclonal antibody against LAMP1 H4A3, developed by J. T. August and J. E. K. Hildreth (Johns Hopkins University School of Medicine, Baltimore, MD) was obtained from the Developmental Studies Hybridoma Bank (Iowa City, IA), developed under the auspices of NICHD, National Institutes of Health and maintained by the University of Iowa (Iowa City, IA). Goat anti-mouse and anti-rabbit coupled to peroxidase (Sigma) were used at a 10^{-4} dilution. Secondary antibodies (donkey anti-rabbit, anti-rat, or anti-mouse IgG conjugated to fluorescein isothiocyanate, Texas red, or cyanine 5 from Jackson ImmunoResearch and goat anti-rabbit and anti-mouse IgG conjugated to Alexa Fluor 350 from Molecular Probes) were used at a 5×10^{-3} dilution.

Gene Cloning and Plasmid Construction—Truncated sequences *sifA*-(1–140), -(36–140), -(71–140), and -(105–140) were amplified by PCR using the forward oligonucleotides O-201, -420, -421, or -422, respectively, and the reverse oligonucleotide O-419. Forward and reverse oligonucleotides were used to introduce EcoRI and BamHI restriction sites, respectively. The PCR products were cloned into the pGEM-T easy vector (Promega). Plasmids for expression of C-terminally GFP-tagged proteins were constructed by digestion of the pGEM-T easy derivate vectors with EcoRI and BamHI and ligation into similarly digested pEGFP-N1 (Clontech). Sequences of *sseJ*-(1–150) was amplified by PCR using oligonucleotides O-276 and O-277. The PCR product was cloned into the pGEM-T easy and subcloned into EcoRI- and SalI-digested pCMV-Myc (Clontech). The full *sifA* open reading frame was amplified by PCR from *S. typhimurium* 12023 genomic DNA using the oligonucleotides O-201 and O-203. The PCR product was subcloned in-frame with GFP into the EcoRI- and XmaI-digested pEGF-N1 generating p*sifA*::GFP. pHA::*skip* was constructed by XhoI and NotI digestion of KIAA0842 cDNA (cloned in pBluescript II SK+, generously provided by Dr. T. Nagase) and cloning into pCMV-HA (Clontech). pGFP::*skip*-(762–885) was constructed by digestion with EcoRI and SalI of pGST::*skip*-(762–885) (12) and cloning into pEGFP-C3 vector (Clontech). SifA mutants were generated by site-directed mutagenesis using a QuikChange kit (Stratagene), and plasmids pDONR::*sifA*, p*sifA*::GFP, pHis::*sifA*, and V-254 (p*sifA*::2HA) as templates (Table 1), and primers O-456 to O-466 (listed in Table 2). The following plasmids were constructed using the Gateway Technology (Invitrogen, Carlsbad, CA). Sequence of SifA-(1–326) open reading frame was amplified by PCR from *S. typhimurium* 12023 genomic DNA with the oligonucleotides SifA1F and SifA327R (Table 2). Orthologous sequence of SifA were amplified by PCR from *S. enterica* s3015 and s2983 genomic DNAs with the oligonucleotide pairs SifA1F-SifA327R and SifA1F2-SifA327R2. The sequence of the SKIP(PH)-(771–878) was amplified from pBluescript II SK+/KIAA0842 with the oligonucleotides SKIP771F and SKIP878R. In all cases, His_6 tag was introduced in the forward oligonucleotides. Sequences of full gene *sifA*, *sifA*-(1–140), and *sifA*-(141–336), were amplified by PCR from *S. typhimurium* 12023 genomic DNA with the oligonucleotides O-299/O-300, O-337/O-338, and O-202/O-343, respectively. PCR products were cloned by recombination into pDONR201 or pDONRzeo vectors. The entry clones were then transferred into Gateway destination vectors, pDEST14, for prokaryotic expression and pCMV-MycGW (12) and pDEST15 for eukaryotic expression.

Protein Purification Protocols—For expression of His-tagged proteins, the plasmids pHis::*sifA*, pHis::*sifA*(s2983), pHis::*sifA*(s3015), pHis::*skip*(PH), and pHis::*sifA*-(1–141) were transformed into *E. coli* C41 (DE3) (Avidis). The cysteine-rich membrane-anchoring region of SifA (15) was deleted. SKIP(PH) was expressed as a minimal domain that encompasses residues 771–878. Protein expression was induced with 0.1 mM isopropyl 1-thio-β-D-galactopyranoside at $A_{600\,nm}$ of 0.5–0.8. After growing for another 8 h at 20 °C, cells were harvested, washed, and resuspended in buffer A (50 mM Tris-HCl, pH 7.6, 300 mM NaCl) and disrupted by sonication, and the lysate was centrifuged at 20,000 $\times$ *g* for 30 min at 4 °C. The supernatant was applied to a nickel-nitrilotriacetic acid-agarose affinity column (Qiagen), pre-equilibrated with buffer A supplemented with 20 mM imidazole. Bound His_6-tagged proteins were eluted with buffer A containing 250 mM imidazole. His-tagged proteins were dialyzed overnight against 10 mM Tris, pH 7.6, 150 mM NaCl, and 1 mM dithiothreitol and loaded onto an Superdex S-75 column (Amersham Biosciences). Fractions were analyzed

TABLE 1
Bacterial strains and plasmids

Bacterial strain or plasmid	Description	Source or reference
***Salmonella* strains**		
12023	Parental strain	(36)
DH215sc4	Δ*sifA*	(8)
PH011	Δ*sifA*, p*sifA*-2HA	(12)
LD101	Δ*sifA*, p*sifA*(L130D)-*2HA*	This study
LD102	Δ*sifA*, p*sifA*(W*XXX*A)-2HA	This study
LD103	Δ*sifA*, p*sifA*(A*XXX*E)-2HA	This study
LD104	Δ*sifA*, p*sifA*(A*XXX*A)-2HA	This study
***E. coli* strains**		
DH5α	F⁻ f80*lacZ*DM15 D(*lacZYA-argF*)*U169 endA1 recA1 hsdR17 deoR supE44 thi-1 gyrA96 relA1*	(37)
BL21 λ (DE3)	F⁻ *ompT* rB⁻ mB⁻ (DE3)	(38)
C41 λ (DE3)	F⁻ *ompT* rB⁻ mB⁻ (DE3) modified	Avidis
Plasmids		
pGEX-4T2	GST in eukaryotic cells	Pharmacia
pEGFP-C1	GFP in eukaryotic cells	Clontech
pKH3-HA$_3$-RhoA	3HA::RhoA in eukaryotic cells	(39)
pKH3-HA$_3$-RhoAN19	3HA::RhoAN19 in eukaryotic cells	(39)
pKH3-HA$_3$-RhoAL63	3HA::RhoAL63 in eukaryotic cells	(39)
pGST::SKIP(PH)(762–885)	GST::SKIP(PH) in *E. coli*	(12)
pMyc::SKIP	Myc::SKIP(PH) in eukaryotic cells	(12)
pSifA::GFP	SifA::GFP in eukaryotic cells	This study
pGST::SifA	GST::SifA in *E. coli*	This study
pGFP::SKIP(PH)	GFP::SKIP(PH) in eukaryotic cells (pEGFP-C3)	This study
pGFP::SifA-(1–140)	GFP::SifA-(1–140) in eukaryotic cells (pEGFP-C1 derivate)	Ruiz-Albert and Holden
pGFP::SifA-(41–336)	GFP::SifA-(41–336) in eukaryotic cells (pEGFP-C1 derivate)	Ruiz-Albert and Holden
pGFP::SseJ-(1–150)	GFP::SseJ-(1–150) in eukaryotic cells (pEGFP-C1 derivate)	Ruiz-Albert and Holden
pMyc::SifA-(1–140)	Myc::SifA-(1–140) in eukaryotic cells	This study
pMyc::SifA-(41–336)	Myc::SifA-(141–336) in eukaryotic cells	This study
pMyc::SseJ-(1–150)	Myc::SseJ-(1–150) in eukaryotic cells	This study
pCMV-HA::SKIP	HA::SKIP in eukaryotic cells	This study
pDONR-His::SifA	His::SifA, Gateway entry clone	This study
pDONR-His::SKIP(PH)	SKIP(PH), Gateway entry clone	This study
pDONR-His::SifA(6)	SifA(s2985), Gateway entry clone	This study
pDONR-His::SifA(9)	SifA(s3015), Gateway entry clone	This study
pHis::SifA	His::SifA in *E. coli*	This study
pHis::SKIP(PH)-(771–878)	His::SKIP(PH) in *E. coli*	This study
pHis::SifA(6)	His::SifA(s2983) in *E. coli*	This study
pHis::SifA(9)	His::SifA(s3015) in *E. coli*	This study
pSifA-(1–39)::GFP	SifA-(1–39)::GFP in eukaryotic cells	This study
pSifA-(1–75)::GFP	SifA-(1–75)::GFP in eukaryotic cells	This study
pSifA-(1–105)::GFP	SifA-(1–105)::GFP in eukaryotic cells	This study
pSifA-(1–140)::GFP	SifA-(1–140)::GFP in eukaryotic cells	This study
pSifA-(36–140)::GFP	SifA-(36–140)::GFP in eukaryotic cells	This study
pSifA-(71–140)::GFP	SifA-(71–140)::GFP in eukaryotic cells	This study
pSifA-(106–140)::GFP	*sifA*-(106–140)::GFP in eukaryotic cells	This study

by SDS-PAGE and mass spectrometry. Proteins were concentrated by ultrafiltration through a PM-10 or PM-5 membrane (Amicon) and stored at 4 °C for a short period of time, or at −80 °C.

Crystallization and Data Collection—Initial crystallization conditions were found from the Crystal Screen (Hampton Research) screen using vapor diffusion in 96-well Greiner plates and a Genesis workstation (Tecan) and a Honeybee robot (Genomic solutions). Optimized conditions for crystallization of the SifA-SKIP(PH) complex (5 mg/ml) at 20 °C used a protein-to-well solution ratio of 3:1, in 30% polyethylene glycol 4000, 0.2 M sodium acetate trihydrate, 0.1 M Tris-HCl, pH 8. Crystals were briefly transferred to the mother liquor supplemented with 20% glycerol and flash-cooled in liquid nitrogen. Data were processed and merged with XDS (22) and scaled with the CCP4 program suite (23).

Structure Solution and Refinement—The structure of the SifA-SKIP(PH) complex was solved by molecular replacement with MOLREP (23) using the homologous structure of the SifA-SKIP(PH) complex (3CXB) (18) as a search model. The model was refined with REFMAC, including TLS refinement. The resulting electron density maps were used, when well defined, to correct the backbone traces along the SifA and SKIP(PH) molecules and position side chains using COOT (24). TLS groups were manually generated and correspond to SifA residues 21–136 and 137–327, and SKIP(PH) residues 772–876. The average root mean square deviation between the final structure and 3CXB is 0.68 Å for 402 Cα atoms. Missing or weak electron densities correspond to SifA surface loops Pro^{168}–Pro^{172}, Arg^{190}–His^{193} and Leu^{244}–Thr^{254} and SKIP(PH) Tyr^{787}–Lys^{790}. The stereochemistry of the structure was analyzed with MolProbity (25). Data collection and refinement statistics are summarized in Table 3.

GST Pulldown and Co-immunoprecipitation Assays, Growth and Bacterial Infection of Tissue Culture Cells, and Mouse Mixed Infections—These experiments were performed as previously described (12).

Scoring of Phenotypes by Epifluorescence Microscopy—Cells were immunolabeled as previously described (8). SCVs and Sifs were labeled by using antibodies against LAMP1- and 2HA-tagged SifA. Infected cells were observed by epifluorescence, and the percentage of GFP-expressing bacteria present in a vac-

TABLE 2
Oligonucleotides used in this study

Oligonucleotide	Sequence (5′ to 3′)
SifA1F	GGGGACAAGTTTGTACAAAAAAGCAGGCTTCGAAGGAGATGCCACCATGAAACATCACCATCACCATCACCCGATTACTATAGGGAATGG
SifA327R	GGGGACCACTTTGTACAAGAAAGCTGGGTTTATTATTGTTCTGAGCGAACGTG
SKIP771F	GGGGACAAGTTTGTACAAAAAAGCAGGCTTCGAAGGAGATGCCACCATGAAACATCACCATCACCATCACACCATCACCAAAGAAGGCATG
SKIP878R	GGGGACCACTTTGTACAAGAAAGCTGGGTTTATCAGGGGATGACCCCTTTGG
SifA1F2	GGGGACAAGTTTGTACAAAAAAGCAGGCTTCGAAGGAGATGCCACCATGAAACATCACCATCACCATCACCCGATCACAATAGGGAATGG
SifA327R2	GGGGACCACTTTGTACAAGAAAGCTGGGTTTATTATAAAAAACCCCTAATCTG
O-201	AAAAAAGAATTCCACCATGCCGATTACTATAGGGAATGG
O-202	AAAAAACCCGGGCTAAAAAACAACATAAACAGCCGC
O-203	CGGATATATTCGCATGGTG
O-276	AAAAGAATTCTCCCATTGAGTGTTGGACAGGG
O-277	AAACAGCTGTTAGTCGCCAAAAAATACCAGTCTGG
O-299	GGGGACAAGTTTGTACAAAAAAGCAGGCTTCCCGATTACTATAGGGAATGGT
O-300	GGGGACCACTTTGTACAAAGCTGGGTCCTATATAAAAAACAACATAAACAGCCGC
O-337	GGGGACCACTTTGTACAAGAAAGCTGGGTCCTACGATTTTAAAATATCCGGGCG
O-338	GGGGACAAGTTTGTACAAAAAAGCAGGCTTCCCGATTACTATAGGGAATGGTTTT
O-343	GGGGACAAGTTTGTACAAAAAAGCAGGCTTCCATCCACAAATGACGGCC
O-344	GGGGACCACTTTGTACAAGAAAGCTGGGTCCTAGCCGCTTTGTTGTTCTGA
O-419	TCATTGGATCCCGCGATTTTAAAATATCCGGGCGATC
O-420	AAAAAAGAATTCCACCATGGACTTCTTTTTTTCTACT
O-421	AAAAAAGAATTCCACCATGGAGTTGAAAGAGTTAGCCTG
O-422	AAAAAAGAATTCCACCATGGAGAACGAATTGTTACGTATC
O-426	TGCTTTTGGATCCCGAAAAAAGAAGTCTTTAATTTTTTC
O-427	TGCGATGGATCCCGTAACTCTTTCAACTCAAAAAAAATC
O-429	TAACAATGGATCCCGTTCGTTTTGATCCATGATGCGAAG

uole was determined by counting the total number of bacteria and the number of bacteria totally or partially encircled by the LAMP1 marker. Sifs and the percentage of SCV-positive for kinesin-1 was determined by visualizing GFP-expressing bacteria in the green channel, LAMP1 in the UV channel, and SifA or kinesin HC in the red channel.

RESULTS

Delineation of the Minimal Domain of SifA That Interacts with SKIP—In infected cells, SifA binds to the C-terminal PH domain of the host protein SKIP, SKIP(PH) (12), and we previously observed that SifA and SKIP interact and co-localize on vesicular clusters when expressed in HeLa cells.[6] Thus the N- and C-terminal domains of SifA (Fig. 1*A*) were tested for their capacity to confer a similar phenotype. Analysis of co-transfected cells showed that the N-terminal but not the C-terminal region of SifA co-localized with SKIP on peripheral vesicular clusters (Fig. 1*B*). Effectors of the *Salmonella*-translocated effectors family harbor similar N-terminal translocation signal domains (13). For example, the first 110 amino acid residues of SseJ share 30% sequence identity and 48% similarity with SifA. However, the N-terminal domain of SseJ was not able to co-localize with SKIP (Fig. 1*B*). We next examined whether this co-localization resulted from a physical interaction. SKIP(PH) immunoprecipitated SifA and SifA-(1–140) but not SifA-(141–336) nor SseJ-(1–150) (Fig. 1*C*). We further examined the ability of the N-terminal domain of SifA to initiate complex formation with SKIP(PH) *in vitro*. Upon mixing of purified His_6::SifA-(1–141) and His_6::SKIP(PH), a protein complex was eluted by size-exclusion chromatography (supplemental Fig. S1, *A* and *B*). Altogether these results clearly indicate that the N-terminal domain of SifA is necessary and sufficient to interact with SKIP(PH).

To delineate the minimal functional domain of SifA sufficient to interact with SKIP, C-terminally GFP-tagged deletions variants were constructed (Fig. 1*A*), expressed in HeLa cells, and analyzed for their ability to be pulled down by GST::SKIP(PH) or GST. SifA and GFP alone were used as positive and negative controls, respectively. Among the tested constructs, SKIP(PH) specifically pulled down full-length SifA and SifA-(36–140) (Fig. 1*D*). Consistently, co-immunoprecipitation experiments revealed that Myc::SKIP co-immunoprecipitated with full-length SifA and SifA-(36–140) (data not shown). Strikingly, SifA-(1–140)::GFP showed no or very weak interaction with SKIP(PH) in the pulldown assay (Fig. 1*D*) and co-immunoprecipitation experiments (data not shown), whereas in HeLa cells it co-localized with Myc::SKIP (data not shown) as efficiently as GFP::SifA-(1–140) (Fig. 1*B*). Altogether, these observations indicate that the N-terminal region of SifA is sufficient to target the PH domain of the host protein SKIP and that the first 35 amino acid residues are not absolutely essential to drive this interaction.

Stoichiometry and Binding Affinity of the SifA-SKIP(PH) Complex—SifA lacking the cysteine-rich membrane anchoring region and SKIP(PH) (residues 771–878) were expressed as His_6 N-terminal fusion proteins in *E. coli*. GST::SKIP(PH) and GST::SifA were able to specifically pull down His_6::SifA and His_6::SKIP(PH), respectively (data not shown), and the individual partners behave as monomers in solution as revealed by size-exclusion chromatography (supplemental Fig. S1*C*). When the partners were mixed prior to injection, a single peak was observed with an estimated mass of 47.8 kDa, nearly corresponding to the molecular mass of a 1:1 SifA-SKIP(PH) complex as verified by SDS-PAGE (supplemental Fig. S1, *C* and *D*) and mass spectrometry (data not shown).

The dissociation constant of the complex was calculated to be 5.7×10^{-6} M by isothermal titration calorimetry measurements (supplemental Fig. S1*E*). Thermodynamic binding parameters were also determined for the interaction between His_6::SKIP(PH) and two SifA orthologs from *Salmonella enterica* s3015 (SARC9) and s2983 (SARC6) that share 92 and 62% sequence identity with SifA from *S. typhimurium* strain

[6] A. Dumont and S. Méresse, unpublished observations.

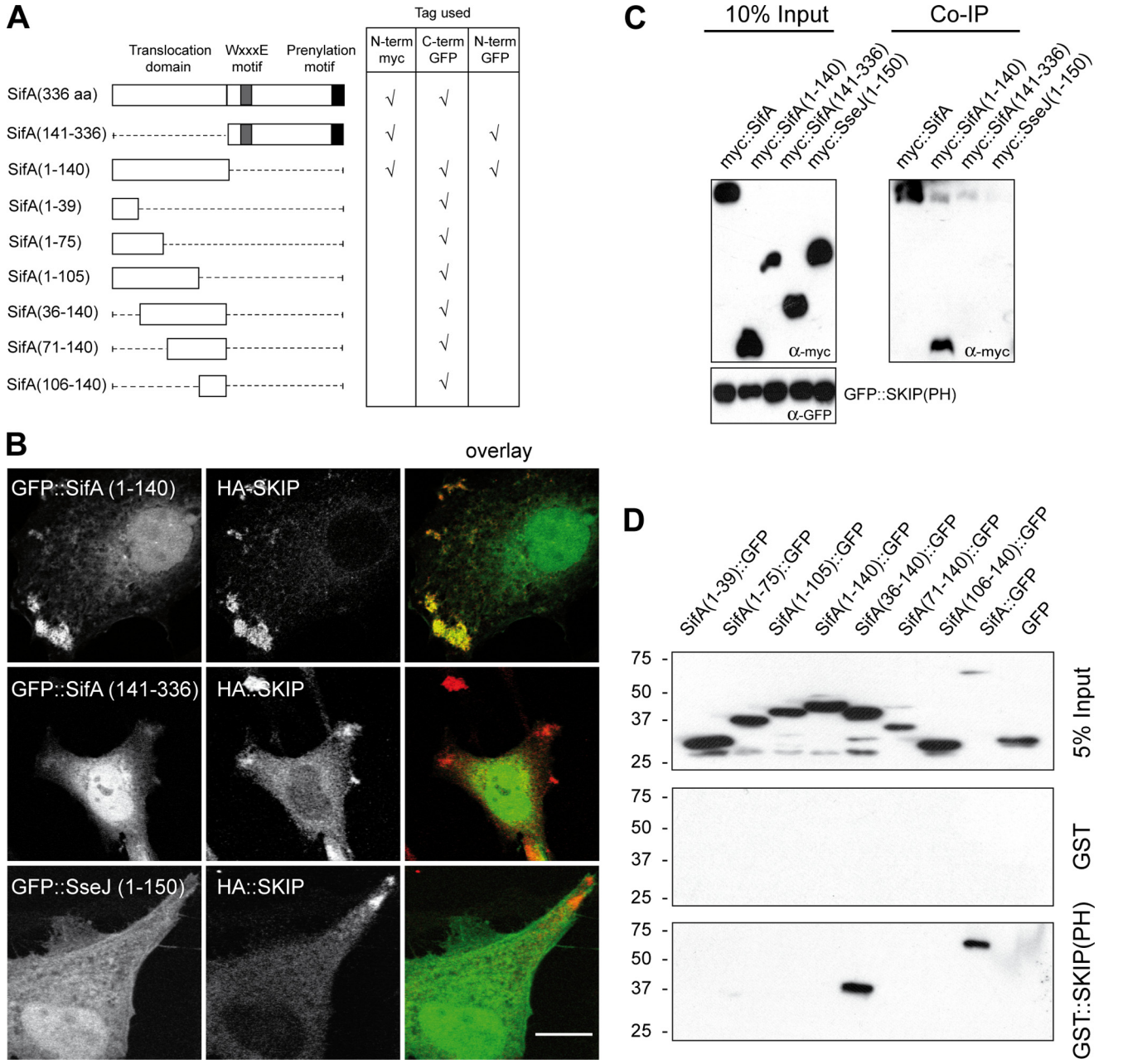

FIGURE 1. **The N-terminal domain of SifA interacts with the PH domain of SKIP.** *A*, schematic representation of SifA and the truncated constructs used in this study and the location of the Myc or GFP fusion tags. *B*, intracellular localization of SifA-derived polypeptides and SKIP. HeLa cells expressing HA::SKIP and GFP::SifA-(1–140), GFP::SifA-(141–336), or GFP::SseJ(1–150) were immunostained for HA. Confocal images show GFP fusion polypeptides (*green*) and HA::SKIP (*red*) (*scale bar*: 10 μm). *C*, SKIP(PH) immunoprecipitates the N-terminal domain of SifA. Cell lysates prepared from HeLa cells expressing GFP::SKIP(PH) and Myc::SifA, Myc::SifA-(1–140), Myc::SifA-(141–336), or Myc::SseJ-(1–150) were incubated with rabbit anti-GFP antibody and Protein A beads. Co-immunoprecipitated proteins were analyzed by Western blotting with an anti-Myc antibody. *D*, GST::SKIP(PH) pulls down SifA-(36–140)::GFP. GST::SKIP(PH) or GST were immobilized on beads and incubated with extracts of HeLa cells expressing GFP, SifA::GFP, and various SifA truncated variants fused to the N terminus of GFP. Bound proteins were analyzed by Western blotting with an anti-GFP antibody.

12023, respectively (supplemental Fig. S2*A*). In each case, comparable dissociation constants were determined. The SifA-SKIP(PH) molecular ratios were calculated as 1:1.53, 1:1.09, and 1:1.28 for SifA from strains 12023, SARC9, and SARC6, respectively, arguing for a 1:1 complex, consistent with the size-exclusion chromatography data.

Overall Structure of the SifA-SKIP(PH) Complex—The structure of the SifA-SKIP(PH) complex was solved at 3.3-Å resolution (Table 3). It validated a 1:1 stoichiometry complex and confirmed the presence of two separate domains of SifA with the N- and C-terminal domains that encompass residues 1–136 and 137–330, respectively. Overall, the SifA-SKIP(PH) structure was similar to the homologous structure of the complex reported previously (18) and emphasized the fact that SKIP(PH) binding is exclusively mediated by the N-terminal domain of SifA (Fig. 2). The binding interface involves 16 residues from each partner and is dominated by the extended β-sheet structure held by four hydrogen bonds involving backbone atoms of SifA Tyr^{128}, Leu^{130}, and Lys^{132}, and SKIP(PH) Gly^{828}, Cys^{830}, and Arg^{831}. Van der Waals interactions (SifA

TABLE 3
Data collection and refinement statistics

	SifA-SKIP(PH)
Data collection	
ESRF beamline	ID14–EH4
Wavelength (Å)	0.939
Space group	$P2_12_12$
Cell dimensions: a, b, c (Å)	91.80, 110.87, 44.27
Resolution range (Å)[a]	47.4–3.3
Total observations	31,607
Unique reflections	7,176
Multiplicity	4.4 (3.7)
Completeness (%)	99.3 (95.8)
R_{sym} (%)[b]	9.1 (41.0)
$\langle I/\sigma(I)\rangle$	8.9 (3.0)
Refinement	
Resolution (Å)	20-3.3
No. reflections	6,424
R_{work}/R_{free} (%)[c]	24.0/30.9
No. atoms (SifA/SKIP(PH))	3,302 (2,488/814)
Average *B*-factors (Å^2), SifA/SKIP(PH) (main to side)	50.9-50.8/49.4-49.5
r.m.s.d.[d]	
Bond (Å)	0.009
Angles (°)	1.34
Chiral volume (A^3)	0.097
Ramachandran plot (%)	
Most favored regions	85.1
Additionally allowed regions	14.7
PDB accession code	3HW2

[a] Values in parentheses are those for the last shell.
[b] $R_{merge} = \Sigma_{hkl\Sigma i}|I_{i(hkl)} - \langle I_{hkl}\rangle|/\Sigma_{hkl\Sigma i}I_{i(hkl)}$, where I is an individual reflection measurement and $\langle I\rangle$ is the mean intensity for symmetry-related reflections.
[c] $R_{cryst} = \Sigma_{hkl}||F_o| - |F_c||/\Sigma_{hkl}|F_o|$, where F_o and F_c are observed and calculated structure factors, respectively. R_{free} is calculated for 9.8% of randomly selected reflections excluded from refinement.
[d] Root mean square deviation from ideal values.

Leu^{127} and Leu^{130} and SKIP(PH) Cys^{870}, Met^{866}, and Val^{873}) are central to the interface while polar interactions (SifA Glu^{24}, Lys^{132}, and Arg^{134} and SKIP(PH) Arg^{831}, Arg^{832}, and Glu^{859}) may serve as boundary clamps for the complex (Fig. 2).

A DALI structure-based search did not reveal any homolog for the N-terminal domain of SifA. In contrast, the C-terminal domain showed a structural similarity with the *Salmonella* effector SopE as previously reported (18). The T3SS-2 effector SifB shares high similarity with SifA along the entire sequence (26% identical and 45% similarity) but does not bind SKIP(PH) (12). Interestingly, SifA residues buried at the complex interface are not conserved in SifB (Fig. 2). In contrast, the critical residues are conserved in the two SifA orthologs SARC6 and SARC9 (supplemental Fig. S2). Mapping residue differences between SifA and SifB onto the surface of SifA showed a marked variability within the C-terminal domain arguing for a different C-terminal-mediated function between these two homologous effectors (Fig. 2*C*). SifA exhibits a strong electropositive patch clustered at the outer convex surface formed by helices α1 and α2 in the N-terminal domain that might facilitate the translocation process or be involved in the interaction with a yet unknown ligand (Fig. 2*D*).

Like other PH domain, the β-sandwich fold of SKIP(PH) is composed of a four-stranded twisted antiparallel β-sheet that packs against a tripled-stranded β-sheet. One end of the β-sandwich is capped by an α-helix that along with the adjacent β7 strand shapes the SifA binding site whereas the opposite face is formed by three loops known to mediate interaction with phosphoinositides (26).

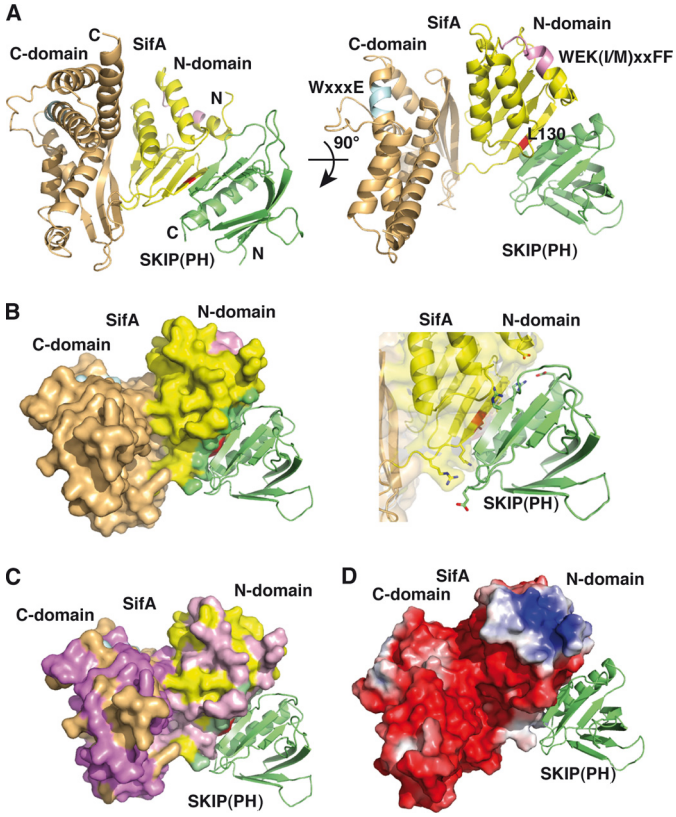

FIGURE 2. **Overall view of the SifA-SKIP(PH) complex.** *A*, *ribbon diagram* of the SifA-SKIP(PH) complex, viewed in two orientations rotated by 90°. The SifA N- (residues 21–136) and C-terminal (residues 137–328) are shown in *yellow* and *orange*, respectively, and the SKIP(PH) (residues 772–876) is in *green*. The SifA conserved motifs WE(I/M)*XX*FF, which is important for translocation (13), and W*XXX*E, which has been proposed to mimic activated GTPase (16), are highlighted in *pink* and *cyan*, respectively. The Leu^{130} position buried at the complex interface is displayed in *red*. *B*, molecular surface of the complex (*left*), color-coded, and oriented as in the *left view* of *panel A*, with the surface buried at the complex interface shown in *green*. Close-up view (*right*) of key residues involved in the binding interface. *C*, mapping sequence conservation in the SifB homolog onto the molecular surface of SifA (*yellow* and *orange* for the N- and C-terminal domain), oriented as in the *left view* of *panel A*, with non-conserved side chains from the N- and C-terminal domain shown in *pink* and *magenta*, respectively. Small patches of non-conserved surface regions (*pink*) are located in the N-terminal domain and within the binding interface (*green*) while large patches of non-conserved surface regions (*magenta*) are clustered within the C-terminal domain. *D*, surface electrostatic potential map of SifA, oriented as in the *right view* of *panel A*, showing a dominant electronegative potential except for a large patch of electropositive potential clustered near the translocation motif in the N-terminal domain. Electrostatic surface potentials are contoured at −3/+3 kT/e electrostatic units (k, Boltzmann constant; T, temperature in Kelvin; e, electronic charge), where *red* describes a negative and *blue* a positive potential. The figures were generated with PyMOL (DeLano Scientific (2004), San Carlos, CA), and *panel D* was generated with the APBS plug-in for PyMOL.

Translocation and SKIP Binding Analysis of Point Mutants of SifA—Our biochemical and structural data indicate that the interaction with SKIP(PH) is mediated only by the N-terminal domain of SifA and is unlikely to involve the W*XXX*E motif localized in the C-terminal domain. These results also suggest that the two domains of SifA could independently contribute to its virulence activity. To decipher which of the SKIP binding or GTPase mimicry domains of SifA mediate the functions of this effector, we engineered point-mutation variants of SifA. Three mutants of the W*XXX*E motif with the tryptophan 197, the glutamic 201, or both replaced by alanine (A*XXX*E, W*XXX*A, and A*XXX*A) were constructed. Furthermore, a structure-

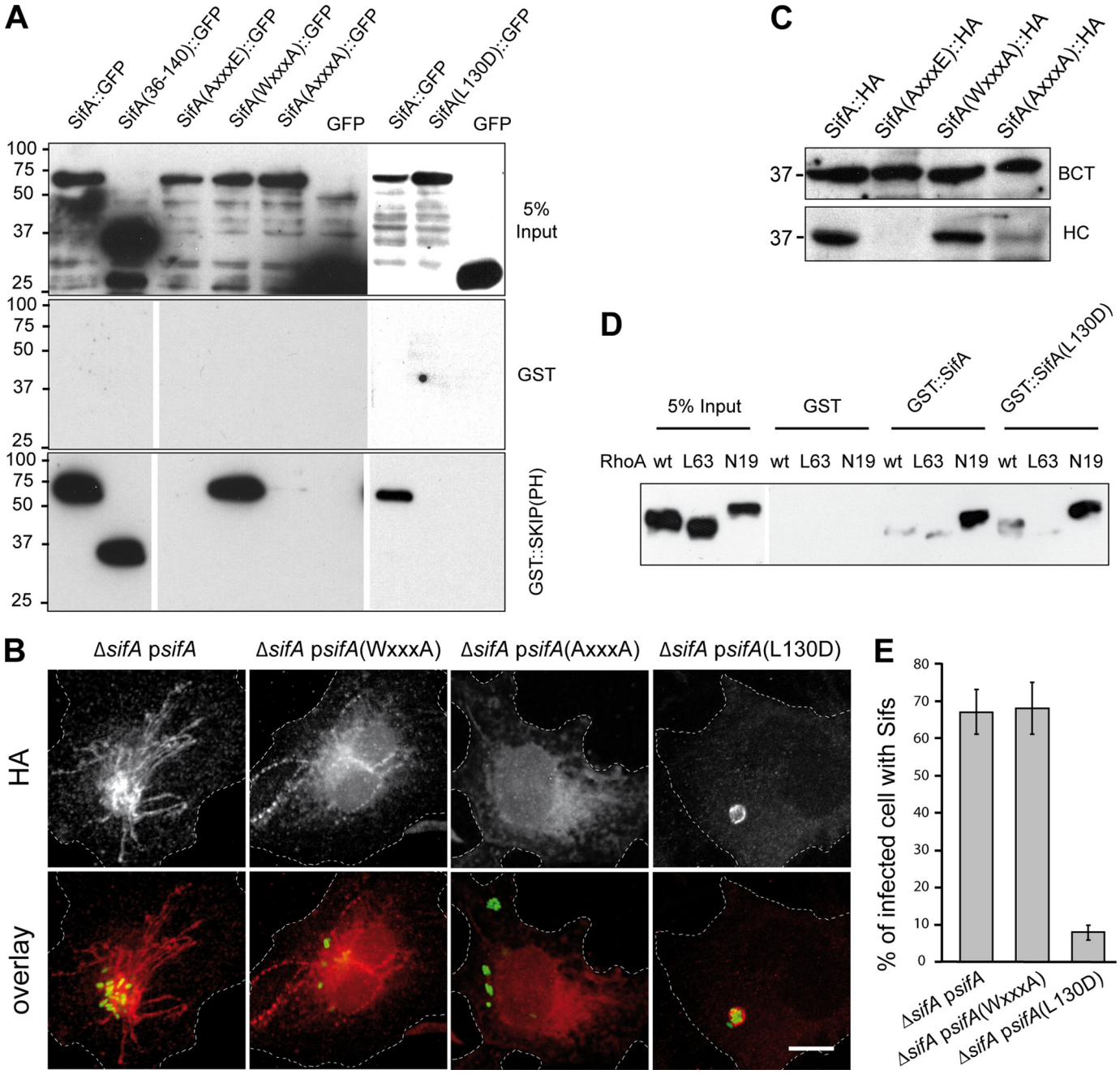

FIGURE 3. **Biochemical and functional analysis of point mutants of SifA: interaction with SKIP and RhoA, translocation, and formation of Sifs.** *A*, pulldown analysis of the interaction between SKIP(PH) and SifA variants. GST::SKIP(PH) or GST were immobilized on beads and incubated with extracts of HeLa cells expressing SifA, SifA-(36–140), or SifA variants (A*XXX*E, W*XXX*A, A*XXX*A, and L130D) fused to the N terminus of GFP or GFP alone. Bound proteins were analyzed by Western blotting with an anti-GFP antibody. *B* and *C*, translocation analysis. HeLa cells were infected for 16 h with Δ*sifA* strains expressing GFP and 2HA-tagged version of wild-type or point-mutation variants of SifA. Cells were either fixed, immunolabeled for HA, and imaged by confocal microscopy for GFP (*green*) and HA (*red*) (*scale bar*, 10 μm) (*B*) or subjected to Triton X-100 extraction and differential centrifugation and analyzed by Western blotting for HA-tagged proteins in bacterial (*BCT*) and HeLa cell (*HC*) fractions (*C*). *D*, both SifA and SifA-(L130D) pull down GDP-bound RhoA. GST::SifA, GST::SifA-(L130D), or GST were immobilized on beads and incubated with extracts of HeLa cells expressing HA-tagged wild-type, GTP-bound (*L63*), or GDP-bound (*N19*) forms of RhoA. Pulled down proteins were analyzed by Western blotting with an anti-HA antibody. *E*, SifA-(L130D) does not support the formation of Sifs. HeLa cells were infected for 16 h, immunostained, and scored for the formation of HA-labeled Sifs.

based mutant for the interaction with SKIP(PH) was made in which we substituted the interacting leucine 130 by an aspartic (L130D). As expected, the SifA-(W*XXX*A) mutant, expressed in HeLa cells as GFP fusion, interacted with SKIP(PH) *in vitro*, whereas SifA-(L130D) did not (Fig. 3*A*). Unexpectedly, the two tryptophan mutants, SifA-(A*XXX*E) and SifA-(A*XXX*A), were also defective in binding to SKIP(PH) (Fig. 3*A*). To get further insights into the functional consequences of these point mutations we used Δ*sifA Salmonella* strains carrying plasmids for the expression of 2HA-tagged SifA (12) bearing the different mutations and looked for *trans* complementation in infected tissue culture cells. Microscopy observations of immunolabeled infected HeLa cells revealed a localization on SCVs for SifA-(L130D) and on SCVs and Sifs for wild-type SifA and SifA-

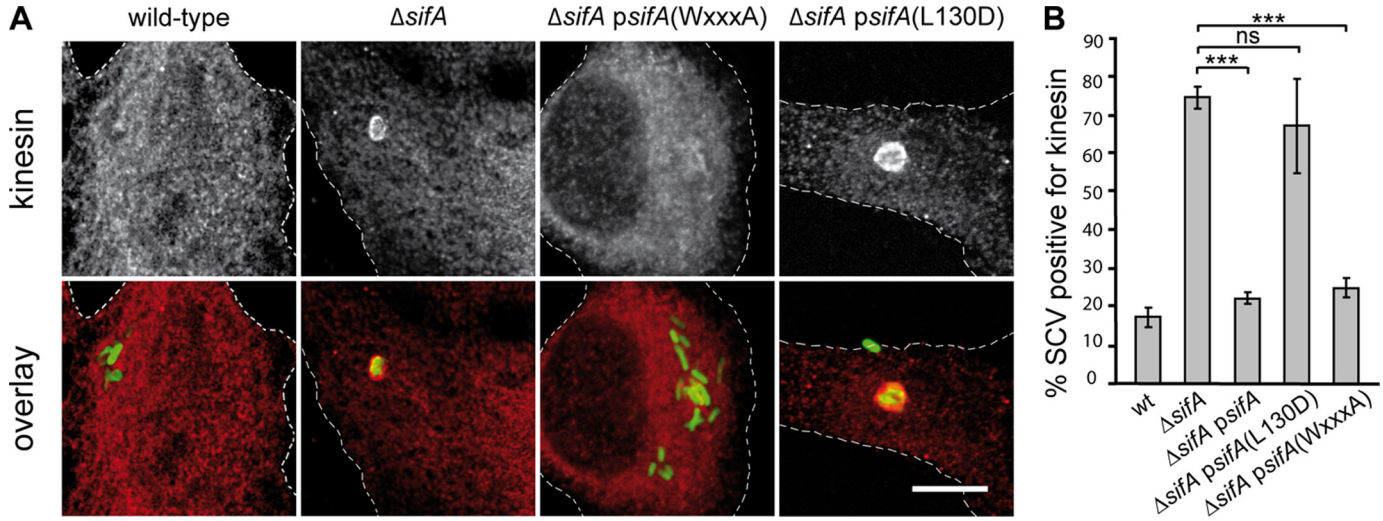

FIGURE 4. **Analysis of point mutants of SifA: accumulation of kinesin on SCVs.** HeLa cells were infected for 16 h with GFP-*Salmonella* strains expressing or not the 2HA-tagged version of wild-type or point-mutation variants of SifA, fixed, immunostained for kinesin HC. Infected cells were imaged by confocal microscopy for GFP (*green*) and kinesin (*red*) (*scale bar*, 10 μm) (*A*) or scored for the percentage of kinesin-positive SCVs (*B*). Values represent the means ± S.D. of three independent experiments, $n = 50$ infected cells for each experiment. *p* values were calculated for cells infected with a complemented strain compared with cells infected with the Δ*sifA* mutant. ***, $p \leq 0.005$; *ns*, $p > 0.05$.

(W*XXX*A) (Fig. 3*B*). However, we could not detect SifA-(A*XXX*A) (Fig. 3*B*) nor SifA-(A*XXX*E) (data not shown) suggesting that these two mutant forms were either not produced or not translocated. To discriminate between these possibilities we analyzed by Western blotting the distribution of wild-type SifA and mutant versions of the W*XXX*E motif in eukaryotic fractions and bacterial pellets prepared from infected cells. Although the different variants of SifA were expressed at similar levels (Fig. 3*C*), only wild-type SifA and the SifA-(W*XXX*A) mutants were recovered from the cellular fraction at substantial and comparable levels. No or a very weak translocation was observed for SifA-(A*XXX*E) and SifA-(A*XXX*A). These results, together with the fact that tryptophan mutants do not interact with SKIP, suggest that stability and/or tertiary structure of tryptophan mutants is altered. Indeed, the crystal structure revealed that the conserved W*XXX*E motif is located at the beginning of helix α6 with Trp^{197} deeply buried within the hydrophobic core of SifA while Glu^{201} is only moderately solvent-exposed and stabilizes the α7–α8 loop.

We further verified that point mutations of SifA that abolished the interaction with SKIP were not affecting its capacity to interact with RhoA (18). N-terminally GST-tagged versions of SifA were analyzed for their ability to pull down HA-tagged RhoA variants. SifA, SifA-(L130D) (Fig. 3*D*), and SifA-(L127D) (data not shown) specifically pulled down RhoA and preferentially in its GDP-bound form. Together these results indicate that SifA interacts independently with RhoA and SKIP.

Analysis of Point Mutants of SifA: Sifs Formation and Kinesin-1 Accumulation—Translocated mutant forms of SifA were further investigated for their capacity to restore a wild-type phenotype in infected HeLa cells. First, expression of SifA or the W*XXX*A mutant restored the formation of Sifs in a Δ*sifA* background as shown by formation of HA-labeled Sifs (Fig. 3, *B* and *E*). In contrast, only a marginal number of Sifs was detected in HeLa cells infected with the strain expressing SifA-(L130D) (Fig. 3, *B* and *E*). We also scored infected HeLa cells for the accumulation of kinesin-1 on the vacuole. An efficient *trans* complementation was observed for strains expressing SifA and SifA-(W*XXX*A), because, like with the wild-type strain, <25% of kinesin-1-positive SCV were scored (Fig. 4, *A* and *B*). Conversely, ~75 and 65% of vacuoles enclosing the Δ*sifA* mutant or the strain expressing SifA-(L130D) accumulated kinesin-1, respectively (Fig. 4, *A* and *B*). These results indicate that SifA-(L130D) is not capable of complementing the Δ*sifA* strain for the formation of Sifs and for the modulation of kinesin-1 recruitment.

Analysis of Point Mutants of SifA: Stability of the Vacuole, Replication in Macrophages, and Virulence in the Mouse Model—Deletion of sifA leads to a marked instability of the vacuole and, as consequences, a replication defect in macrophages (7) and an attenuation of virulence in mice (27). We investigated whether point-mutated forms of SifA would complement these phenotypes. No improvement in the stability of the vacuolar membrane and a modest increase in the capacity to replicate in RAW264.7 mouse macrophages were observed for the SifA-(L130D) mutant (Fig. 5, *A* and *B*). In contrast, expression of SifA or SifA-(W*XXX*A) stabilized the vacuole and increased the bacterial replication in tissue culture macrophages. To address whether the expression of these SifA variants would rescue the virulence of a Δ*sifA* mutant, we injected C57BL/6 mice intraperitoneally with 10^5 cfu of a 1:1 mix of Δ*sifA* and another strain. Bacteria were recovered from mouse spleens after 2 days, and the competitive index was determined (28). Like the wild-type strain, Δ*sifA*p*sifA* and Δ*sifA*p*sifA*(W*XXX*A) were significantly more virulent than Δ*sifA* (Fig. 5*C*). In contrast, expression of SifA-(L130D) did not significantly change the virulence activity of the Δ*sifA* strain. Altogether these results demonstrate that the W*XXX*A mutation did not affect the function of SifA, whereas the L130D mutation abolished its function (Fig. 5). They show that formation of the SifA-SKIP complex is required to mediate SifA functions. They also indicate that other signaling or interacting motifs are, in the context of this experimental

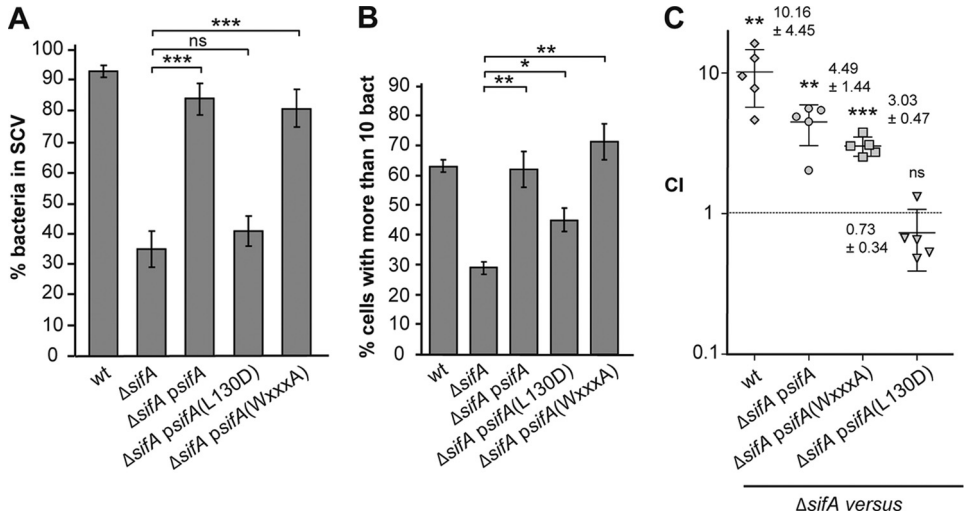

FIGURE 5. **Analysis of point mutants of SifA: stability of the vacuole, replication in macrophages, and virulence in mice.** *A*, HeLa cells were infected for 16 h with GFP-*Salmonella* strains expressing or not the 2HA-tagged version of wild-type or point-mutation variants of SifA, fixed, and immunostained for the SCV marker LAMP1. Percentages of bacteria in SCVs were scored. *B*, infected RAW 264.7 mouse macrophage cells were infected for 16 h, fixed, and examined by epifluorescence microscopy for enumeration of intracellular bacteria. Percentages of infected cells in which bacteria replicated (cells with >10 bacteria) were determined. *A* and *B*, results are the average of three independent experiments in which >50 cells were scored. *p* values are indicated and were obtained by comparing indicated strains. *C*, mice were inoculated intraperitoneally with a mixture of two strains. At day 2 after injection, spleens were harvested for bacterial counts. Competitive indexes of Δ*sifA* against wild-type *Salmonella* or Δ*sifA* strains expressing wild-type or point-mutation variants of SifA were determined. Each *symbol* represents the competitive index from one mouse, and *horizontal bars* correspond to the mean ± S.D. of all of the mice, as indicated. *ns*, $p > 0.05$; *, $p \leq 0.05$; **, $p \leq 0.01$; and ***, $p \leq 0.001$.

study, either not active or acting downstream of the SifA-SKIP complex formation.

DISCUSSION

The translocation of SifA in infected cells has numerous consequences on the host-pathogen interplay and impacts the virulence of *Salmonella*. In infected cells SifA interacts with the host protein SKIP. However, it has been unclear whether this interaction controls every SifA-associated phenotype. SifA displays multiple domains and motifs, of which some have been proposed to act independently of the interaction with SKIP (18). We used biochemistry and crystallography to delineate the SifA-SKIP interaction domains and show that all known phenotypes associated with the expression of SifA are dependant on its interaction with SKIP.

We have solved a crystal structure of the SifA-SKIP(PH) complex that is very homologous to the one reported (18). Biochemical data indicate that the first 140 residues of SifA are sufficient to interact directly with the PH domain of SKIP. We also establish that the first 36 residues of SifA, which are mostly disordered until Asn^{21} before helix α1 (residues Trp^{26}–Phe^{37}), are not strictly required for this interaction *in vitro*, albeit Glu^{24} and Trp^{26} that mediate interactions with SKIP(PH) at the periphery of the complex interface most probably weakly contribute to complex stability.

We made use of Δ*sifA* strains expressing wild-type or mutant forms of SifA from a plasmid to investigate the functionality and the physiological outcomes of important motifs. The distal end of the N-terminal domain of SifA binds SKIP(PH), and residues Leu^{127} and Leu^{130} participate in the complex interface with SKIP(PH). Consequently, mutants SifA-(L127D) (data not shown) and SifA-(L130D) have lost the capacity to form a complex with SKIP. Also, we introduced point mutations in the W*XXX*E motif present in a large group of bacterial effectors that were suggested to function as mimics of GTPases (16). In infected tissue culture cells and in the mouse model of infection, Δ*sifA* strains expressing SifA-(L130D) demonstrated phenotypes similar as those observed in the absence of the effector. In contrast, identical phenotypes were observed for the strains expressing SifA-(W*XXX*A) or the wild-type effector. The invariant tryptophan and glutamic residues of the W*XXX*E motif are both important for the activity of the *Shigella* effector protein IpgB2 (16). Therefore, one would expect that a strain expressing SifA-(W*XXX*A) would, at least to some extent, behave like a Δ*sifA* strain if this motif would be functionally important. Because strains expressing mutant forms of SifA that do not interact with SKIP behave like a Δ*sifA* mutant, we propose that SifA activities are mediated by or are downstream of the interaction with SKIP.

The C-terminal piece of SifA has a fold similar to the early *Salmonella* effector SopE (18). SopE is a guanine nucleotide exchange factor (29). Consistently, SifA was found to bind RhoA in its GDP-bound form, but purified SifA failed to show any guanine nucleotide exchange activity for this GTPase (18). SifA and the late endosomal GTPase Rab9 were established to bind competitively to the PH domain of SKIP (30). The same study has involved the W*XXX*E motif of SifA in this interaction. Yet, we and other (18, 30) also observed that mutation of the tryptophan residue in the W*XXX*E motifs of SifA impedes the interaction with SKIP(PH) *in vitro*. In contrast, SifA bearing a mutation of the glutamic residue (W*XXX*A) was still able to interact. Analysis of these mutants in infected tissue culture cells demonstrated that SifA-(A*XXX*E) and SifA-(A*XXX*A) were normally synthesized but not translocated. Attempts to purify these SifA variants revealed unstable proteins that tended to precipitate. In SifA, residue Trp^{197} is not exposed to the solvent and is located in a wide zone of hydrophobic contacts, being essential for the local structural integrity. In contrast, Glu^{201} may also stabilize helix-8 by hydrogen-bonding and hydrophobic contacts. Therefore, it is very likely that the A*XXX*E and A*XXX*A mutant forms of SifA do not favor a stable tertiary structure and prevent interaction with SKIP. A recent analysis also demonstrated that small truncations all through SifA are sufficient to block its secretion and/or translocation, suggesting that a completely intact SifA is required for these processes (31). We propose that, in SifA, the W*XXX*E stretch is

a structural motif, which is not directly implicated in the function of this effector but is essential for the stability and the conformation of the protein.

The interaction between purified SifA and SKIP(PH) analyzed by calorimetry presents a dissociation constant of 5.7×10^{-6} M, a modest affinity for an intracellular protein-protein interaction (32, 33) that is nevertheless sufficient to isolate the complex by size-exclusion chromatography. Because this study was performed using a SKIP-derived peptide restricted to the SifA binding site, we cannot exclude that the complex formed with full-length SKIP presents a lower dissociation constant in physiological conditions. Our result is consistent with the one of Ohlson *et al.* (2.6×10^{-6} M) (18), whereas the binding reported by Jackson *et al.* (30) was significantly stronger (0.2×10^{-6} M). These variations are likely due to the difference in methods and polypeptides used for the measurement. For example, we used an His_6 tag fusion for both proteins in place to use GST (30), which has been reported to induce dimerization (34). *In vivo*, the SifA-SKIP affinity could also be modulated by other eukaryotic protein and/or other TTSS-2 *Salmonella* effectors that may interfere with SifA functions. The effector-mediated modulation of host function is transient and may need to be reversible and/or regulated (35). Hence, the moderate affinity between SifA and SKIP(PH) might allow another effector to prevail over SifA activity at some stage of the infectious process.

Both SifA, through SKIP, and PipB2 bind kinesin-1 (8, 12), but the respective contributions of these effector proteins in the activity of the molecular motor are not yet understood. Both interact with the tetratricopeptide repeat domain of kinesin light chain (8).[6] However, although a direct binding has been demonstrated for PipB2, the kinesin-1-SKIP interaction remains to be characterized. The next challenge will be to better understand the prokaryotic and eukaryotic molecular scaffolds that form upon translocation of *Salmonella* effector proteins and, more specifically, how the SifA-SKIP complex controls the membrane exchanges leading to the formation of stable vacuoles and Sifs that are so crucial for *Salmonella* virulence.

Acknowledgments—We thank Alexandra Vergnes for critical reading of the manuscript and Miguel Ortiz-Lombardia, Silvia Spinelli, and Florence Vincent for helpful discussion on crystallogenesis and structure determination. We thank E. Lemichez, O. Visvikis, J. Ruiz-Albert, and D. W. Holden for their kind gifts of plasmids.

REFERENCES

1. Levine, W. C., Buehler, J. W., Bean, N. H., and Tauxe, R. V. (1991) *J. Infect Dis.* **164,** 81–87
2. Tsolis, R. M., Kingsley, R. A., Townsend, S. M., Ficht, T. A., Adams, L. G., and Bäumler, A. J. (1999) *Adv. Exp. Med. Biol.* **473,** 261–274
3. Steele-Mortimer, O. (2008) *Curr. Opin. Microbiol.* **11,** 38–45
4. Poh, J., Odendall, C., Spanos, A., Boyle, C., Liu, M., Freemont, P., and Holden, D. W. (2008) *Cell Microbiol.* **10,** 20–30
5. Rytkönen, A., Poh, J., Garmendia, J., Boyle, C., Thompson, A., Liu, M., Freemont, P., Hinton, J. C., and Holden, D. W. (2007) *Proc. Natl. Acad. Sci. U.S.A.* **104,** 3502–3507
6. Mazurkiewicz, P., Thomas, J., Thompson, J. A., Liu, M., Arbibe, L., Sansonetti, P., and Holden, D. W. (2008) *Mol. Microbiol.* **67,** 1371–1383
7. Beuzón, C. R., Méresse, S., Unsworth, K. E., Ruíz-Albert, J., Garvis, S., Waterman, S. R., Ryder, T. A., Boucrot, E., and Holden, D. W. (2000) *EMBO J.* **19,** 3235–3249
8. Henry, T., Couillault, C., Rockenfeller, P., Boucrot, E., Dumont, A., Schroeder, N., Hermant, A., Knodler, L. A., Lecine, P., Steele-Mortimer, O., Borg, J. P., Gorvel, J. P., and Méresse, S. (2006) *Proc. Natl. Acad. Sci. U.S.A.* **103,** 13497–13502
9. Méresse, S., Unsworth, K. E., Habermann, A., Griffiths, G., Fang, F., Martínez-Lorenzo, M. J., Waterman, S. R., Gorvel, J. P., and Holden, D. W. (2001) *Cell Microbiol.* **3,** 567–577
10. Salcedo, S. P., and Holden, D. W. (2003) *EMBO J.* **22,** 5003–5014
11. Ramsden, A. E., Mota, L. J., Münter, S., Shorte, S. L., and Holden, D. W. (2007) *Cell Microbiol.* **9,** 2517–2529
12. Boucrot, E., Henry, T., Borg, J. P., Gorvel, J. P., and Méresse, S. (2005) *Science* **308,** 1174–1178
13. Miao, E. A., and Miller, S. I. (2000) *Proc. Natl. Acad. Sci. U.S.A.* **97,** 7539–7544
14. Reinicke, A. T., Hutchinson, J. L., Magee, A. I., Mastroeni, P., Trowsdale, J., and Kelly, A. P. (2005) *J. Biol. Chem.* **280,** 14620–14627
15. Boucrot, E., Beuzón, C. R., Holden, D. W., Gorvel, J. P., and Méresse, S. (2003) *J. Biol. Chem.* **278,** 14196–14202
16. Alto, N. M., Shao, F., Lazar, C. S., Brost, R. L., Chua, G., Mattoo, S., McMahon, S. A., Ghosh, P., Hughes, T. R., Boone, C., and Dixon, J. E. (2006) *Cell* **124,** 133–145
17. Freeman, J. A., Ohl, M. E., and Miller, S. I. (2003) *Infect Immun.* **71,** 418–427
18. Ohlson, M. B., Huang, Z., Alto, N. M., Blanc, M. P., Dixon, J. E., Chai, J., and Miller, S. I. (2008) *Cell Host Microbe* **4,** 434–446
19. Miroux, B., and Walker, J. E. (1996) *J. Mol. Biol.* **260,** 289–298
20. Vincentelli, R., Canaan, S., Offant, J., Cambillau, C., and Bignon, C. (2005) *Anal. Biochem.* **346,** 77–84
21. Dumont, A., Schroeder, N., Gorvel, J. P., and Méresse, S. (2007) *Methods Mol. Biol* **394,** 275–287
22. Kabsch, W. (1993) *J. Appl. Crystallogr.* **26,** 795–800
23. Collaborative Computational Project, N. (1994) *Acta Crystallogr D. Biol. Crystallogr* **50,** 760–763
24. Emsley, P., and Cowtan, K. (2004) *Acta Crystallogr D. Biol. Crystallogr* **60,** 2126–2132
25. Davis, I. W., Leaver-Fay, A., Chen, V. B., Block, J. N., Kapral, G. J., Wang, X., Murray, L. W., Arendall, W. B., 3rd, Snoeyink, J., Richardson, J. S., and Richardson, D. C. (2007) *Nucleic Acids Res.* **35,** W375–W383
26. Lemmon, M. A. (2004) *Biochem. Soc. Trans.* **32,** 707–711
27. Stein, M. A., Leung, K. Y., Zwick, M., Garcia-del Portillo, F., and Finlay, B. B. (1996) *Mol. Microbiol.* **20,** 151–164
28. Beuzón, C. R., and Holden, D. W. (2001) *Microbes Infect.* **3,** 1345–1352
29. Hardt, W. D., Chen, L. M., Schuebel, K. E., Bustelo, X. R., and Galán, J. E. (1998) *Cell* **93,** 815–826
30. Jackson, L. K., Nawabi, P., Hentea, C., Roark, E. A., and Haldar, K. (2008) *Proc. Natl. Acad. Sci. U.S.A.* **105,** 14141–14146
31. Brown, N. F., Szeto, J., Jiang, X., Coombes, B. K., Finlay, B. B., and Brumell, J. H. (2006) *Microbiology* **152,** 2323–2343
32. Nooren, I. M., and Thornton, J. M. (2003) *J. Mol. Biol.* **325,** 991–1018
33. Nooren, I. M., and Thornton, J. M. (2003) *EMBO J.* **22,** 3486–3492
34. Lim, K., Ho, J. X., Keeling, K., Gilliland, G. L., Ji, X., Rüker, F., and Carter, D. C. (1994) *Protein Sci.* **3,** 2233–2244
35. Patel, J. C., and Galán, J. E. (2005) *Curr. Opin. Microbiol.* **8,** 10–15
36. Wray, C., and Sojka, W. J. (1978) *Res. Vet. Sci.* **25,** 139–143
37. Hanahan, D. (1983) *J. Mol. Biol.* **166,** 557–580
38. Studier, F. W., and Moffatt, B. A. (1986) *J. Mol. Biol.* **189,** 113–130
39. Boyer, L., Turchi, L., Desnues, B., Doye, A., Ponzio, G., Mege, J. L., Yamashita, M., Zhang, Y. E., Bertoglio, J., Flatau, G., Boquet, P., and Lemichez, E. (2006) *Mol. Biol. Cell* **17,** 2489–2497